Coherent Control of a Single Trapped Rydberg Ion

Gerard Higgins,[1,2,*] Fabian Pokorny,[1] Chi Zhang,[1] Quentin Bodart,[1] and Markus Hennrich[1]
[1]Department of Physics, Stockholm University, SE-106 91 Stockholm, Sweden
[2]Institut für Experimentalphysik, Universität Innsbruck, AT-6020 Innsbruck, Austria
(Received 13 September 2017; published 28 November 2017)

Trapped Rydberg ions are a promising novel approach to quantum computing and simulations. They are envisaged to combine the exquisite control of trapped ion qubits with the fast two-qubit Rydberg gates already demonstrated in neutral atom experiments. Coherent Rydberg excitation is a key requirement for these gates. Here, we carry out the first coherent Rydberg excitation of an ion and perform a single-qubit Rydberg gate, thus demonstrating basic elements of a trapped Rydberg ion quantum computer.

DOI: 10.1103/PhysRevLett.119.220501

Systems of trapped ion qubits have set numerous benchmarks for single-qubit preparation, manipulation, and readout [1]. They can perform low-error entanglement operations [2,3] with up to 14 ion qubits [4]. Still, a major limitation towards realizing a large-scale trapped ion quantum computer or simulator is the scalability of entangling quantum logic gates [5].

Arrays of neutral atoms in dipole traps offer another promising approach to quantum computation and simulation. Here, qubits are stored in electronically low-lying states and multiqubit gates may be realized by exciting atoms to Rydberg states [6–9]. Rydberg states are exotic states of matter in which the valence electron is excited to high principal quantum numbers. They can have extremely high dipole moments and may interact strongly with each other, which has allowed entanglement generation [10,11] and fast two-qubit Rydberg gates [12] in neutral atom systems.

A system of trapped Rydberg ions may combine the advantages of both technologies. Electronically low-lying states may be used as qubit states and fast multiqubit gates are envisaged by coherently exciting ions to Rydberg states and employing dipolar interactions between them [13,14]. Multiqubit gates commonly used in trapped ion systems suffer scalability restrictions due to the spectral crowding of motional modes [5]. This issue does not affect multiqubit Rydberg gates and thus a trapped Rydberg ion quantum computer offers an alternate approach to a scalable system.

An unanswered question was whether trapped ions can be excited to Rydberg states in a coherent fashion as is required for multiqubit Rydberg gates. In this work we perform coherent Rydberg excitation of a single trapped ion by stimulated Raman adiabatic passage (STIRAP) with a $(91 \pm 3)\%$ transfer efficiency. We combine coherent Rydberg excitation by STIRAP with qubit manipulation to demonstrate a single-qubit Rydberg phase gate. We perform process tomography of the gate with a π phase shift and measure $(78^{+4}_{-8})\%$ fidelity. This indicates our system is capable of implementing a two-qubit Rydberg gate (as proposed in Ref. [15]) using dipolar interactions between microwave-dressed Rydberg states [13,14]; thus, a trapped Rydberg ion quantum computer may be feasible.

In our experiment we study a single $^{88}Sr^{+}$ ion confined in a linear Paul trap. Three atomic levels in a ladder configuration are coupled using two UV lasers (Fig. 1). The qubit state $|0\rangle$ is coupled to the excited state $|e\rangle$ by the pump laser at 243 nm with Rabi frequency Ω_P. $|e\rangle$ is coupled in turn to the Rydberg state $|r\rangle$ $(42S_{1/2}, m_J = -1/2)$ using the Stokes laser at 307 nm with Rabi frequency Ω_S. The experimental setup is described in detail in the Supplemental Material [16] and in Ref. [24]. In our experiment we carry out two-photon Rydberg excitation; in another experiment trapped

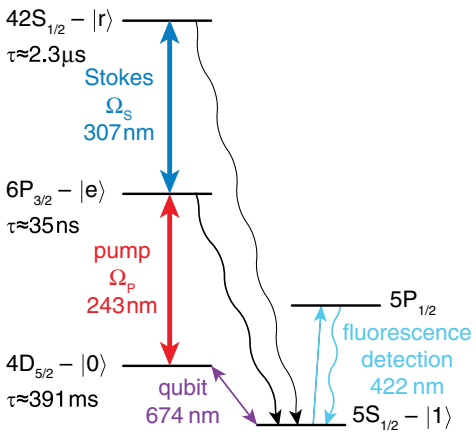

FIG. 1. Three atomic levels of $^{88}Sr^{+}$ are coupled by two UV lasers. The qubit state $|0\rangle$ is coupled to $|e\rangle$ by the pump laser; $|e\rangle$ is coupled to the Rydberg state $|r\rangle$ using the Stokes laser. Population in $|e\rangle$ or $|r\rangle$ decays mostly to $5S_{1/2}$; detection of scattered fluorescence light heralds excitation from $|0\rangle$ and decay to $5S_{1/2}$. Transitions between the qubit states are driven by a laser at 674 nm. Initialization is described in detail in the Supplemental Material [16]. The lifetimes of $|r\rangle$ and $|0\rangle$ [23] differ by 5 orders of magnitude and thus Rydberg states are envisaged for use in qubit manipulation rather than for storing qubits.

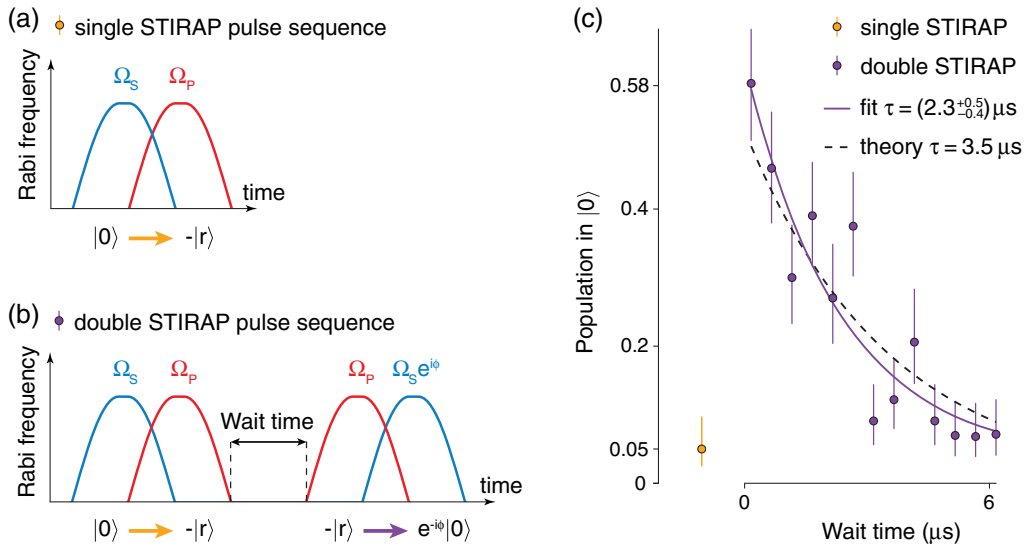

FIG. 2. Coherent Rydberg excitation by STIRAP shown by comparing the application of the single and the double STIRAP pulse sequences. After the single STIRAP pulse sequence, shown in (a), $(5^{+5}_{-2})\%$ of the population remains in $|0\rangle$, as shown in (c); the rest of the population is transferred to $5S_{1/2}$ via $|r\rangle$ or $|e\rangle$. After the double STIRAP pulse sequence, shown in (b), most of the population may lie in $|0\rangle$, as in (c), which shows population is transferred successfully to the Rydberg state $|r\rangle$ and returned to $|0\rangle$. By varying the wait time between the two sets of STIRAP pulses the Rydberg state lifetime is measured. Error bars indicate projection noise (68 % confidence interval). The evolution of the dark state $|\Phi_{\text{dark}}\rangle$ is described beneath each pulse sequence.

Rydberg ions are produced by a single vacuum ultraviolet–photon excitation [25,26].

We can use the two-photon coupling for coherent control of the Rydberg excitation. At two-photon resonance ($|0\rangle$ to $|r\rangle$) the coupling Hamiltonian has a "dark" eigenstate $|\Phi_{\text{dark}}\rangle \sim \Omega_S e^{i\phi}|0\rangle - \Omega_P|r\rangle$ [16], which is named so because it does not contain any component of the lossy state $|e\rangle$ and thus it does not scatter light in time scales much less than τ_{42S}, the lifetime of the Rydberg state $42S_{1/2}$ ($|r\rangle$). The character of the dark state depends on the ratio Ω_S/Ω_P. Thus, by adiabatically varying Ω_S and Ω_P according to the pulse sequence in Fig. 2(a), population initially in $|0\rangle$ follows the evolution of the dark state and is transferred to $-|r\rangle$ without populating $|e\rangle$. This process is called STIRAP. Because STIRAP is immune against loss by spontaneous emission from the intermediate state and it is robust against small variations of experimental conditions [27] we favor this method over two-photon Rabi oscillations.

Laser pulses are shaped by driving acousto-optic modulators using arbitrary waveform generators such that the Rabi frequencies rise and fall in a sinusoidal fashion over time t_{rise} as in Fig. 2. Simulations indicate sinusoidal-shaped pulses yield a higher STIRAP efficiency in our system than Gaussian-shaped pulses [16]. t_{rise} must be long for adiabatic evolution of the state vector; however, it is required to be short to reduce losses from Rydberg state decay and from decoherence due to finite laser linewidths. We find $t_{\text{rise}} = 200$ ns to be a suitable compromise. To maximize the STIRAP efficiency the peak Rabi frequencies of the two lasers are matched [16] and made as high as is experimentally attainable, $\Omega_{\text{peak}} \approx 2\pi \times 47$ MHz. With the sinusoidal pulse shapes and the matched peak Rabi frequencies of the two lasers the adiabaticity criterion $1/4t_{\text{rise}} = 1.25\ \text{MHz} \ll \Omega_{\text{peak}}/2\pi \approx 47\ \text{MHz}$ is satisfied [28]. Both UV laser linewidths are estimated to be $\sim 2\pi \times 100$ kHz and are sufficiently low ($\ll \Omega_{\text{peak}}$, $2\pi/t_{\text{rise}}$) to allow adiabatic following.

Detecting population transfer by STIRAP in our system relies upon discriminating population in the state $5S_{1/2}$ from population in the initial state $|0\rangle$ by detecting fluorescence on the $5S_{1/2} \leftrightarrow 5P_{1/2}$ transition (Fig. 1). After applying the single STIRAP pulse sequence [Fig. 2(a)] $(95^{+2}_{-5})\%$ of the population is transferred out of $|0\rangle$ into $5S_{1/2}$ [Fig. 2(c)]. This is because $> 93\%$ of the population decays from both $|r\rangle$ and $|e\rangle$ to $5S_{1/2}$ by multichannel decay processes in $< \sim 20\ \mu$s [24,29,30]. The time resolution of state detection in our system does not allow us to distinguish successful STIRAP to $|r\rangle$ from simple optical pumping via $|e\rangle$. We therefore apply a double STIRAP sequence that concludes with 58% of the population returned to $|0\rangle$ [Fig. 2(c)], thus demonstrating successful excitation and deexcitation by STIRAP. The return of population is not perfect because the state vector does not perfectly follow the dark state throughout the pulse sequence, due to Rydberg state decay, finite laser linewidths, and a short t_{rise}.

During the wait time in the double STIRAP sequence population may decay from $|r\rangle$ and be removed from the three-level system. By measuring the population returned to $|0\rangle$ as the wait time is varied the lifetime of $|r\rangle$ is determined, $\tau_{42S} = (2.3^{+0.5}_{-0.4})\ \mu$s [Fig. 2(c)] [16]. This is

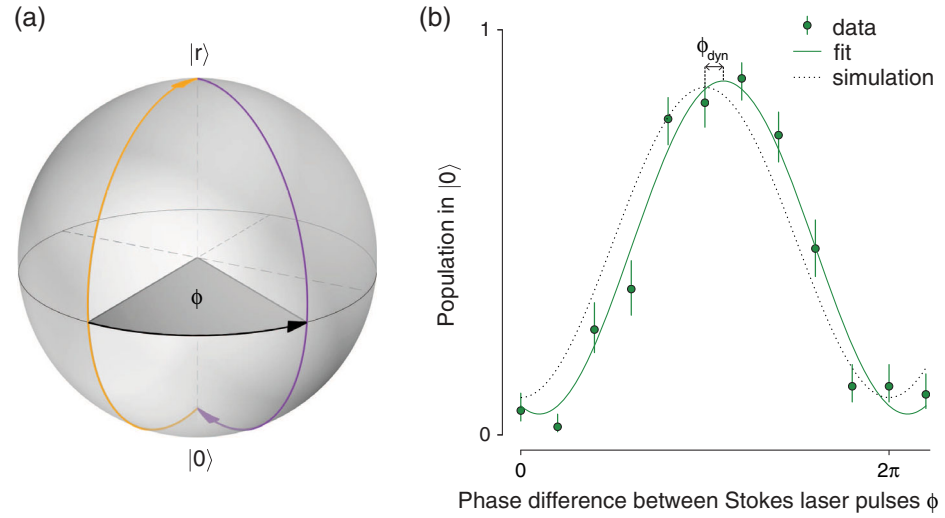

FIG. 3. Accumulation of a geometric phase during the shortened double STIRAP sequence. (a) We control the path traversed by the dark state on the Bloch sphere spanned by $|0\rangle$ and $|r\rangle$ by varying the phase ϕ of the second Stokes pulse [see Fig. 2(b)]. The area enclosed by the path results in the accumulation of a geometric phase $|0\rangle \rightarrow e^{-i\phi}|0\rangle$. (b) The geometric phase is measured in a Ramsey experiment. The shortened double STIRAP sequence is nested between two Ramsey pulses on the 674 nm transition between the qubit states $|0\rangle \leftrightarrow |1\rangle$. As ϕ is varied the final population in $|0\rangle$ oscillates. Error bars indicate projection noise (68 % confidence interval).

the first lifetime measurement of a trapped Rydberg ion. Comparing this with the 3.5 μs theoretically predicted lifetime of $42S_{1/2}$ in free space at 300 K [16] suggests the Rydberg state lifetime is not significantly shortened by confinement in the Paul trap. This is important for trapped Rydberg ions to be a viable quantum technology, since Rydberg state lifetimes place fundamental limits on gate fidelities [7] and resonance linewidths. Since the lifetime of a Rydberg state scales with the core charge Z as Z^{-4} [31] Rydberg ions ($Z = +2$) have lifetimes an order of magnitude lower than neutral Rydberg atoms ($Z = +1$). For high-fidelity Rydberg gates faster excitation to Rydberg states with higher principal quantum numbers ($n \approx 60$) may be employed.

Using a shortened double STIRAP pulse sequence in which a single pump laser pulse is applied between two Stokes laser pulses, as in Fig. 3 in the Supplemental Material [16], $(83^{+5}_{-6})\%$ of the population is returned to $|0\rangle$, which indicates a single STIRAP efficiency of $\sqrt{(83^{+5}_{-6})\%} = (91 \pm 3)\%$. This marks a significant improvement on the highest STIRAP efficiency observed with neutral Rydberg atoms (60%) [32–34].

We use the shortened double STIRAP sequence to introduce a geometric phase following the protocol recently demonstrated with a solid-state qubit [35]. During the shortened double STIRAP sequence, the dark state moves on the surface of the Bloch sphere spanned by $|0\rangle$ and $|r\rangle$ from the $|0\rangle$ pole to the $|r\rangle$ pole then back to $|0\rangle$ [Fig. 3(a)]. When the dark state reaches the $|r\rangle$ pole the phase of the Stokes laser is shifted by ϕ using an acousto-optic modulator, and the dark state returns to the $|0\rangle$ pole along a different Bloch sphere longitude. This "tangerine slice" trajectory with wedge angle ϕ circumscribes a solid angle 2ϕ and gives rise to an accumulated geometric phase of $-\phi$.

This geometric phase is detected by using the other qubit state $|1\rangle$ $(5S_{1/2}, m_J = -\frac{1}{2})$ as a phase reference in a Ramsey experiment. The shortened double STIRAP sequence is nested between two Ramsey pulses on the $|1\rangle \leftrightarrow |0\rangle$ transition at 674 nm. A complete oscillation in the $|0\rangle$ population is observed as ϕ is varied, Fig. 3(b), which shows an arbitrary geometric phase may be acquired. The imperfect STIRAP efficiency and additional decoherence from finite UV laser linewidths cause the contrast of the oscillation, defined as the maximal value minus the minimal value, to be less than unity, $\mathcal{C} = (82 \pm 4)\%$ [16]. Decay of population outside the $\{|0\rangle, |1\rangle\}$ manifold to $5S_{1/2}, m_J = +\frac{1}{2}$ causes the center of the oscillation to be lower than 0.5. This experiment is simulated using the Lindblad master equation with experimentally determined parameters [16]. Excellent agreement is observed between the simulation and the experimental results. The $(18 \pm 4)°$ dynamic phase offset ϕ_{dyn} in the experimental data may be accounted for by small detunings ($\sim 2\pi \times 100$ kHz) of the UV lasers from resonance and the light shift from the Stokes laser acting on $|1\rangle$. The simulated curve displays a lower contrast than the experimental results, which may be accounted for by overestimation of the UV laser linewidths. The simulation predicts a STIRAP efficiency of 90%, limited by Rydberg state decay, UV laser linewidths, and nonadiabaticity in the state evolution during the short rise time. Thus, the efficiency may be improved by increasing the UV laser light intensity at the ion to allow faster adiabatic passage, improving the UV laser frequency stabilization, and exciting higher Rydberg states with longer lifetimes [36].

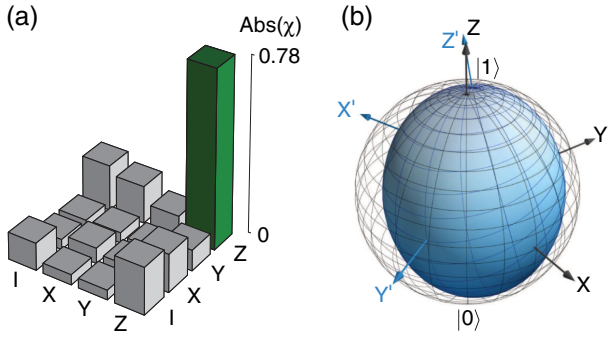

FIG. 4. Process tomography results of the shortened double STIRAP sequence (Fig. 3 in the Supplemental Material [16]) with $\phi = \pi$. (a) The absolute value of the process matrix. The process fidelity $(78^{+4}_{-8})\%$ is the height of the ZZ-bar, which is identical to a σ_z rotation. (b) Reconstructed Bloch sphere after the sequence. In the ideal process the sphere would be rotated about the z axis by π.

The shortened double STIRAP sequence that introduces a geometric phase implements a single-qubit phase gate in the qubit basis. We characterize this operation for $\phi = \pi$, (double STIRAP $|0\rangle \rightarrow -|r\rangle \rightarrow -|0\rangle$) by performing quantum process tomography using a maximum likelihood estimation [16,37,38]. The measured process fidelity is $(78^{+4}_{-8})\%$; the errors are estimated using Monte Carlo simulations. The reconstructed process matrix χ and the postprocess Bloch sphere are plotted in Fig. 4. A perfect operation with a process fidelity of unity would result in a σ_z rotation and the postprocess Bloch sphere would be rotated about the z axis by π. Imperfections in the process cause a shrinking of the $|0\rangle$ pole of the Bloch sphere due to the imperfect STIRAP efficiency and a rotation about the z axis $\neq \pi$ due to a dynamical phase shift. The postprocess Bloch sphere is not symmetric about the z axis because of imperfect Ramsey pulses.

We experimentally realized the coherent Rydberg excitation of a single trapped ion and implemented a single-qubit geometric phase gate in Rydberg excitation and deexcitation. These are basic elements of a trapped Rydberg ion quantum computer. In particular, the single-qubit Rydberg phase gate demonstrated here may be extended to a two-qubit controlled phase gate [15] based on Rydberg interaction [13,14]. The next step is to use microwave radiation to produce Rydberg-S + Rydberg-P superposition states that have large oscillating dipole moments. The dipolar interaction between two Rydberg-S + Rydberg-P ions may be used for a Rydberg gate. Such a gate offers an alternate approach towards a scalable system and may open up a new paradigm for quantum computation.

The research leading to these results has received funding from the European Research Council under the European Union's Seventh Framework Programme/ERC Grant Agreement No. 279508.

*gerard.higgins@fysik.su.se

[1] T. P. Harty, D. T. C. Allcock, C. J. Ballance, L. Guidoni, H. A. Janacek, N. M. Linke, D. N. Stacey, and D. M. Lucas, Phys. Rev. Lett. **113**, 220501 (2014).
[2] C. J. Ballance, T. P. Harty, N. M. Linke, M. A. Sepiol, and D. M. Lucas, Phys. Rev. Lett. **117**, 060504 (2016).
[3] J. P. Gaebler, T. R. Tan, Y. Lin, Y. Wan, R. Bowler, A. C. Keith, S. Glancy, K. Coakley, E. Knill, D. Leibfried, and D. J. Wineland, Phys. Rev. Lett. **117**, 060505 (2016).
[4] T. Monz, P. Schindler, J. T. Barreiro, M. Chwalla, D. Nigg, W. A. Coish, M. Harlander, W. Hänsel, M. Hennrich, and R. Blatt, Phys. Rev. Lett. **106**, 130506 (2011).
[5] C. Monroe and J. Kim, Science **339**, 1164 (2013).
[6] D. Jaksch, J. I. Cirac, P. Zoller, S. L. Rolston, R. Côté, and M. D. Lukin, Phys. Rev. Lett. **85**, 2208 (2000).
[7] M. Saffman, T. G. Walker, and K. Mølmer, Rev. Mod. Phys. **82**, 2313 (2010).
[8] A. Browaeys, D. Barredo, and T. Lahaye, J. Phys. B **49**, 152001 (2016).
[9] M. Saffman, J. Phys. B **49**, 202001 (2016).
[10] T. Wilk, A. Gaëtan, C. Evellin, J. Wolters, Y. Miroshnychenko, P. Grangier, and A. Browaeys, Phys. Rev. Lett. **104**, 010502 (2010).
[11] Y.-Y. Jau, A. M. Hankin, T. Keating, I. H. Deutsch, and G. W. Biedermann, Nat. Phys. **12**, 71 (2016).
[12] L. Isenhower, E. Urban, X. L. Zhang, A. T. Gill, T. Henage, T. A. Johnson, T. G. Walker, and M. Saffman, Phys. Rev. Lett. **104**, 010503 (2010).
[13] M. Müller, L. Liang, I. Lesanovsky, and P. Zoller, New J. Phys. **10**, 093009 (2008).
[14] W. Li and I. Lesanovsky, Appl. Phys. B **114**, 37 (2014).
[15] D. Møller, L. B. Madsen, and K. Mølmer, Phys. Rev. A **75**, 062302 (2007).
[16] See Supplemental Material at http://link.aps.org/supplemental/10.1103/PhysRevLett.119.220501, which includes Refs. [17–22], for further details on the experimental setup, the state preparation, the determination of the UV-laser Rabi frequencies and detunings, the derivation of the dark eigenstate, the choice of the pulse shape, the calculation of the Rydberg state lifetime, the determination of best fit parameters, the Lindblad master equation simulations, the shortened double STIRAP pulse sequence, and quantum process tomography.
[17] E. H. Pinnington, R. W. Berends, and M. Lumsden, J. Phys. B **28**, 2095 (1995).
[18] E. Biémont, J. Lidberg, S. Mannervik, L.-O. Norlin, P. Royen, A. Schmitt, W. Shi, and X. Tordoir, Eur. Phys. J. D **11**, 355 (2000).
[19] J. Johansson, P. Nation, and F. Nori, Comput. Phys. Commun. **184**, 1234 (2013).
[20] I. I. Beterov, M. Saffman, E. A. Yakshina, D. B. Tretyakov, V. M. Entin, G. N. Hamzina, and I. I. Ryabtsev, J. Phys. B **49**, 114007 (2016).
[21] T. F. Gallagher and W. E. Cooke, Phys. Rev. Lett. **42**, 835 (1979).
[22] D. Foreman-Mackey, D. W. Hogg, D. Lang, and J. Goodman, Publ. Astron. Soc. Pac. **125**, 306 (2013).
[23] V. Letchumanan, M. A. Wilson, P. Gill, and A. G. Sinclair, Phys. Rev. A **72**, 012509 (2005).

[24] G. Higgins, W. Li, F. Pokorny, C. Zhang, F. Kress, C. Maier, J. Haag, Q. Bodart, I. Lesanovsky, and M. Hennrich, Phys. Rev. X **7**, 021038 (2017).
[25] T. Feldker, P. Bachor, M. Stappel, D. Kolbe, R. Gerritsma, J. Walz, and F. Schmidt-Kaler, Phys. Rev. Lett. **115**, 173001 (2015).
[26] P. Bachor, T. Feldker, J. Walz, and F. Schmidt-Kaler, J. Phys. B **49**, 154004 (2016).
[27] N. V. Vitanov, A. A. Rangelov, B. W. Shore, and K. Bergmann, Rev. Mod. Phys. **89**, 015006 (2017).
[28] K. Bergmann, N. V. Vitanov, and B. W. Shore, J. Chem. Phys. **142**, 170901 (2015).
[29] H. Zhang, M. Gutierrez, G. H. Low, R. Rines, J. Stuart, T. Wu, and I. Chuang, New J. Phys. **18**, 123021 (2016).
[30] U. I. Safronova, Phys. Rev. A **82**, 022504 (2010).
[31] V. Lebedev and I. Beigman, *Physics of Highly Excited Atoms and Ions* (Springer, Berlin, 1998).
[32] T. Cubel, B. K. Teo, V. S. Malinovsky, J. R. Guest, A. Reinhard, B. Knuffman, P. R. Berman, and G. Raithel, Phys. Rev. A **72**, 023405 (2005).
[33] J. Deiglmayr, M. Reetz-Lamour, T. Amthor, S. Westermann, A. L. de Oliveira, and M. Weidemüller, Opt. Commun. **264**, 293 (2006).
[34] B. M. Sparkes, D. Murphy, R. J. Taylor, R. W. Speirs, A. J. McCulloch, and R. E. Scholten, Phys. Rev. A **94**, 023404 (2016).
[35] C. G. Yale, F. J. Heremans, B. B. Zhou, A. Auer, G. Burkard, and D. D. Awschalom, Nat. Photonics **10**, 184 (2016).
[36] T. F. Gallagher, *Rydberg Atoms* (Cambridge University Press, Cambridge, England, 2005).
[37] I. L. Chuang and M. A. Nielsen, J. Mod. Opt. **44**, 2455 (1997).
[38] D. F. V. James, P. G. Kwiat, W. J. Munro, and A. G. White, Phys. Rev. A **64**, 052312 (2001).